Time dependent Superhydrophobicity of Drag Reducing Surfaces

Musuvathi S. BOBJI*, Ganesh BALAN, Raghuraman N. GOVARDHAN

* Corresponding author: Tel.: ++91 80 2293 3233; Fax: ++91 80 2360 0648 ; Email: bobji@mecheng.iisc.ernet.in
Department of Mechanical Engineering, Indian Institute of Science, Bangalore 560 012, India

Abstract

Air can be trapped on the crevices of specially textured hydrophobic surfaces immersed in water. This heterogenous state of wetting in which the water is in contact with both the solid surface and the entrapped air is not stable. Diffusion of air into the surrounding water leads to gradual reduction in the size and numbers of the air bubbles. The sustainability of the entrapped air on such surfaces is important for many underwater applications in which the surfaces have to remain submersed for longer time periods. In this paper we explore the suitability of different classes of surface textures towards the drag reduction application by evaluating the time required for the disappearance of the air bubbles under hydrostatic conditions. Different repetitive textures consisting of holes, pillars and ridges of different sizes have been generated in silicon, aluminium and brass by isotropic etching, wire EDM and chemical etching respectively. These surfaces were rendered hydrophobic with self-assembled layer of fluorooctyl trichlorosilane for silicon and aluminium surfaces and 1-dodecanethiol for brass surfaces. Using total internal reflection the air bubbles are visualized with the help of a microscope and time lapse photography. Irrespective of the texture, both the size and the number of air pockets were found to decrease with time gradually and eventually disappear. In an attempt to reverse the diffusion we explore the possibility of using electrolysis to generate gases at the textured surfaces. The gas bubbles are nucleated everywhere on the surface and as they grow they coalesce with each other and get pinned at the texture edges.

Keywords: Superhydrophobic Surfaces, Drag reduction, Surface Texturing, underwater hydrophobicity

1. Introduction

Superhydrophobic surfaces with contact angles greater than 150^o have been realized by controlling the surface energy and surface roughness (Callies .and Quere, D 2005; Herminghaus, S. 2000; Bico, J., Marzolin, C., Quere, D. 1999; Yoshimitsu, Z., Nakajima, A., Watanabe, T., Hashimoto, K. 2002; Cao, L., Hu, H.; Gao, D. 2007; Shibuichi, et al. 1996). The water contacts only at the top of the asperities on a fraction of the solid surface (ϕ_s) resulting in a composite 'Cassie state' at the interface (Bico, J., Marzolin, C., Quere, D. 1999). The two main classes of applications of such textured hydrophobic surfaces are the self cleaning applications mimicking lotus leaves and under water applications for drag reduction (Murmur, A. 2006). If the same texture can be used for both the applications then it is better to cover the hulls of the ships with lotus leaves. However, it is a common observation that the lotus leaves retain their non-wetting behaviour when immersed in water for few seconds but lose their superhydrophobicity when the immersion time is in minutes or when subjected to higher water pressure. (Cheng, Y-T., Rodak, D.E. 2005; Zhang,J., Sheng, X., Jiang, L. 2009) Retaining the non-wetting behaviour is one of the main design criteria for underwater applications. We use a visualization technique based on the total internal reflection (TIR) of light at the water-air interfaces to evaluate the air retaining capacities of the surfaces with different types of textures and explore the possibility of active generation of gases on the surfaces using electrolysis.

Slip length is a parameter that quantifies the extent to which a superhydrophobic surface reduces the resistance to the flow of. Slip length (Pierre Joseph, Patrick Tabeling 2005) is defined as the ratio of the velocity of the water layer in contact with the surface (slip velocity) to the velocity gradient at the surface. Larger the slip length lesser the resistance offered by the surface to the flow. Typically the slip length is of the order of few nanometers (Choi, C.; Westin, K.J.A.; K.S. Breuer, K.S. 2003) for the atomically smooth hydrophobic surfaces. On the textured surfaces with 'Cassie state' slip lengths up to few tens of microns have been reported.(Ou, J.; Perot, B.; Rothstein 2004; Truesdell, R. et al.2006; Lee, C. ; Choi, C. ; Kim, C 2008). It is becoming clear that the reason for this large slip length is that the air present on the composite surface offer less resistance compared to the completely wetted 'Wenzel state'.(Govardhan, R.N et al. 2009). This large slip is referred to as apparent slip contrasting the inherent slip that may be resulting from the molecular lever hydrophobic interactions.

Flow over a solid and gas composite surface to the water can be approximated as flow over an alternating no-slip and no-shear regions as the shear resistance offered by air is negligible. Analysis of such a surface shows that the slip length is proportional to the size of the no-shear regions for a given fraction ϕ_s (Lauga, E.; Stone, H.A.;2003). The size of the air bubble that can be sustained under water will depend on the hydrostatic pressure. Typically at 1 m depth the water pressure supported by the radius of the air bubble of size less than 10 microns (Murmur, A. 2006). Thus the maximum slip length that can be obtained will be limited by the depth at which the surface is used.

Air/vapour bubbles in water will shrink in size due to diffusion and the time to disappear will depend on the air saturation level and the surface tension. (Epstein, P.S.; Plesset, M.S 1950; Liebermann, L. 1957) This means that that the apparent slip length of the composite surface will gradually decrease with immersion time (Govardhan, R.N et al. 2009). Very small bubbles may persist (Liebermann, L. 1957) on the suitably shaped crevices on the hydrophobic surfaces however the slip length induced by them will be small. In this paper we report on our experiments visualizing the air bubbles trapped on the immersed hydrophobic surfaces.

2. Experiment

A schematic of the experimental setup we have used is shown in the figure 1. A parallel beam of light is incident on the hydrophobic surface at angle greater than 53^o ($\sin^{-1}(\mu)$) to the normal. If there is an air water interface parallel to the hydrophobic surface then the light will under go TIR and reflected beam would be bright. This effect has been used to detect the presence of the air on the immersed superhydrophobic surfaces previously. (Larmour, I.A.; Bell, S.E.J.; Saunders, G.C. 2007; Sakai, M. et al. 2009; Govardhan, R.N et al. 2009). The reflected light is brought to focus on to a CCD camera with the help of a long working distance microscope. The microscope is focussed on the surface enabling the recording of the air bubbles. For a spherical air-water interface there will be one bright spot for each bubble.

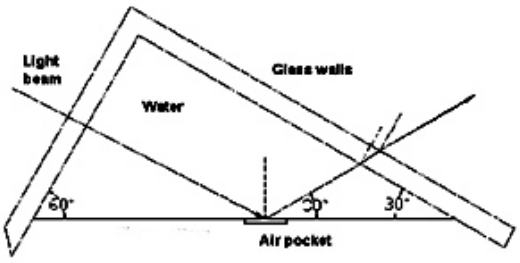

Figure 1 Schematic of Experimental Setup

The CCD camera is programmed to take images at a regular interval of 30 seconds. Using the intensity thresholds and filtering the background of the image is eliminated and he bright spots are counted by identifying the contiguous area of brightness. The variation of the number of the air bubbles present on the surface can then be obtained as a function of

the immersion time from all the images.

The TIR experiments were carried out with deionized water at 25^0C after leaving the water in the lab environment for a minimum of 2 days, such that the water is saturated with air. Bubbling the air through the water overnight did not give any appreciable change in the results obtained. In between two trials, the hydrophobic surfaces were dried and flushed with dry nitrogen for 30 min. This restored the air retention capacity of the surfaces.

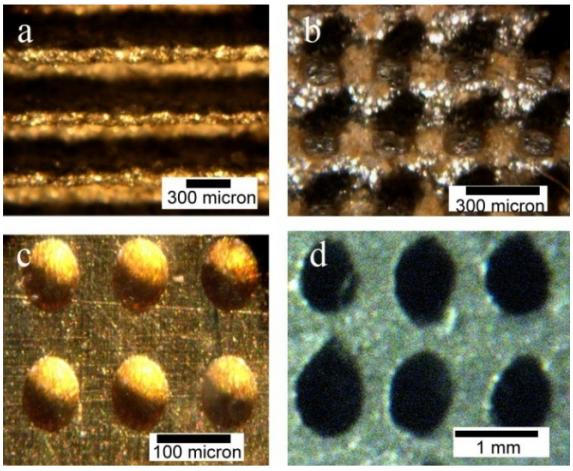

Figure 2 Optical micrograph of various textured surfaces tested. a) Ridges and b) Pillars obtained by EDM in aluminium, c) blind holes in brass generated by chemical etching and d) Holes in Aluminium generated by mechanical drilling.

Five different kinds of surface textures were generated with different geometry/size. A regular array of pillars with square cross section was chosen to mimic the lotus leaf. In an effort to compartmentalize the trapped air pockets, such that any instability in one location would not result in complete loss of the Cassie state, arrays of ridges and holes were also generated. It was hoped that the ridges, mimicking duck feathers would confine the air along one lateral direction while the holes would confine the air in both in plane lateral directions. The surface with the array of square crates/hole can be thought of as a complementary or negative surface to the one with the pillars. The round holes were generated at different sizes owing to their ease of manufacturing using conventional processes.

The first two textures (figure 2 a and b) with a regular array of features, were generated by wire EDM process on aluminium. A wire of 250 micron diameter was used to create the ridges and square pillars of 500 micron depth. The circular through hole of 0.5 mm diameter was fabricated using conventional drilling process on a 2 mm thick aluminium sheet.

The square crates of 30 micron depth was made of a 110 silicon wafer was chosen such that it produced a texture with vertical walls. (M.S.Bobji et al. 2009) The root-mean-square roughness of this polished wafer as measured by using an atomic force microscope was about 0.5 nm. A positive photoresist was spin coated and exposed to UV light for 2.5 s through a photomask. Then the photoresist was developed and the oxide layer was removed with HF to expose the silicon at the desired locations. The anisotropic etching was carried out with a 40% by weight KOH solution at 75^0C. The photomask was oriented with the crystallographic directions of the wafer such that crates were obtained. The 100 micron diameter circular holes were obtained through similar process of photoetching on a brass sheet of 200 micron thickness. The dimensions of the texture produced were measured with a noncontact 3-D optical profilometer (Veeco).

To render the aluminium and silicon surfaces hydrophobic, a self-assembled layer of 1H,1H,2H,2H-perfluorooctyl trichlorosilane (FOTS) was formed from solution. The silicon samples were first cleaned in methanol and then hydrolyzed by soaking in water. The aluminum surfaces were ultrasonicated in a 50:50 deionized water/acetone mixture for 1 h and then cleaned in methanol solution. The surfaces were then dried in an oven at 600C for 1 h, and the samples were stored in a vacuum desiccator.

A mixture of 1 mM FOTS (purity of>98%was obtained from Aldrich Inc.) was prepared in isooctane solvent. The cleaned and hydrolyzed samples were immediately dipped into freshly prepared solution for 1 h. The samples were then taken out, rinsed, and washed with isooctane to remove excess solution.

To render the brass surfaces hydrophobic, the brass surfaces were cleaned and degreased using actone and deionized water respectively. The surfaces were then dipped in a 50mM solution of 1-dodecanethiol in ethanol solvent for 30 minutes. The samples were then taken out, rinsed and dried in an oven kept at 60^0 C.

Contact angles on various surfaces with freshly formed FOTS /thiol were measured with deionized water using image processing techniques. The contact angle on the polished silicon surface without any texture was found to be in the range of 115-120^o.The diamond polished aluminum surface with FOTS layer and brass surface with thiol layer also had a water contact angle in the same range.

3. Results and Discussions

The freshly formed hydrophobic surface was kept in an empty tank, and the water level was slowly raised such that the center of the area observed in the microscope was 6 cm below the final water level. This gave a hydrostatic pressure of about 600 Pa. A slow filling of water ensures that air gets trapped in the texture and there is no premature transition to Wenzel state during the filling.

The images as recorded by the CCD camera at different time intervals are shown in figure 3. The bright spots in these figures correspond to the points on the air-water interface at which the light undergoes total internal reflection. It can be seen that the number of bright spots gradually decreases with time and completely disappear eventually.

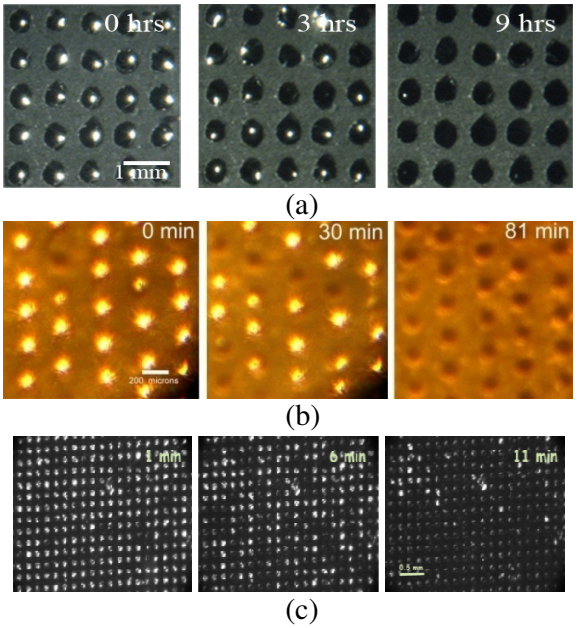

Figure 3 Visualisation of air bubbles at different immersion times on : a) 500 micron holes b)100 micron holes, c) 100 micron square holes / crates

It was found that very little / no bright spots could be seen when the surfaces with pillar and ridges were kept under water. This seem to indicate that these textures are not very good in trapping air initially due to their open structure. However, the surfaces with holes were able to trap air easily, with no air bubbles appearing outside the holes. It can be seen that almost all the holes are filled on immersion and as time passes one by one the holes lose the trapped air. This would mean that either all the air in the hole has disappeared or that air-water interface has moved deep into the hole and thus preventing the reflected light from reaching the microscope. The time taken for each bubble to disappear is quite random.

The number of holes, *N*, that are filled at any point of time with the air normalized with the total number of holes present in the field of view, N_0 is shown in figure 4.

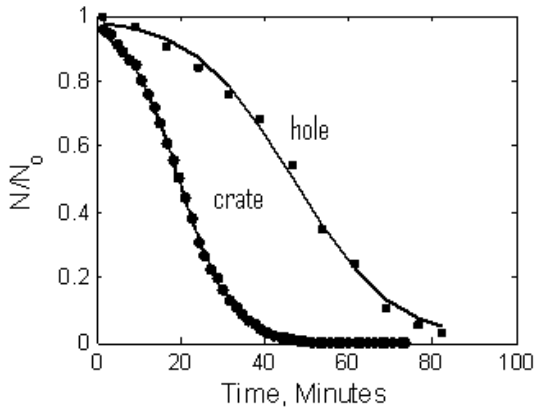

(a)

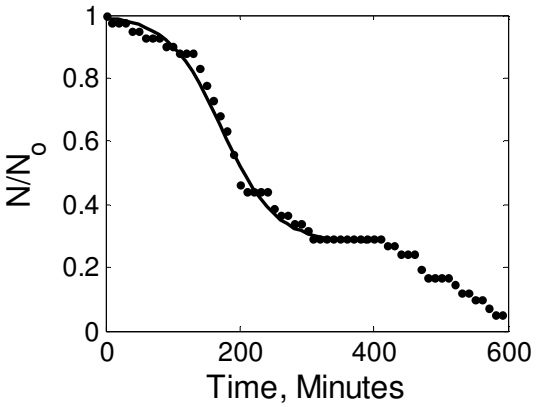

(b)

Figure 4 Variation of the number of bubbles filled with air (normalised) against time (in minutes) for a) 100 micron holes and 100 micron crates b) 500 micron holes

The disappearance of the air bubbles, which could be attributed to diffusion of gases into water over time, seemed to be highly dependent on the size of the bubble. The bubbles in the 500 micron diameter holes (Fig 3a) took 580 minutes as compared to those in the 100 micron diameter holes (Fig 3b) which took 81 minutes.

The result obtained from 100 micron holes is comparable to work done by Epstein-Plesset (1950) who have shown that a spherical bubble of radius 100 micron would take about 98 minutes for complete dissolution through diffusion in a saturated solution. It should be noted that the Epstein-Plesset analysis is for a spherical bubble and in the rough hydrophobic surface as the air diffuses out the meniscus can change from convex to concave shape. Then the pressure in the bubble would be less than the aqueous pressure due to the surface tension effects and thus preventing further diffusion (Liberman 1957).

The shape of the hole seemed to play a major role in the disappearance of bubbles as well. The air bubbles trapped in 100 micron square holes (Fig 3c) were found to diffuse quicker as compared to round holes of similar size as seen in Fig 4a.

The reason for large slip lengths is that the air present on the composite surface offers less resistance compared to the completely wetted 'Wenzel state'.(Govardhan, R.N et al. 2009).This means that the diffusion of bubbles will eventually lead to reduction of slip lengths, and ultimately produce lesser drag reduction. The possibility of using electrolysis of water as a gas generation method to counter this gas diffusion was explored. The time lapse images recorded for the different textures undergoing electrolysis are shown in Fig 5.

For electrolysis, .01M solution of sodium sulphite on water was used as the electrolyte. A voltage of 10V was applied between the textured surface made of aluminium / brass as the cathode and a graphite electrode as the anode. As soon as the electrolytic circuit was closed, the gas generation began on the textured surface.

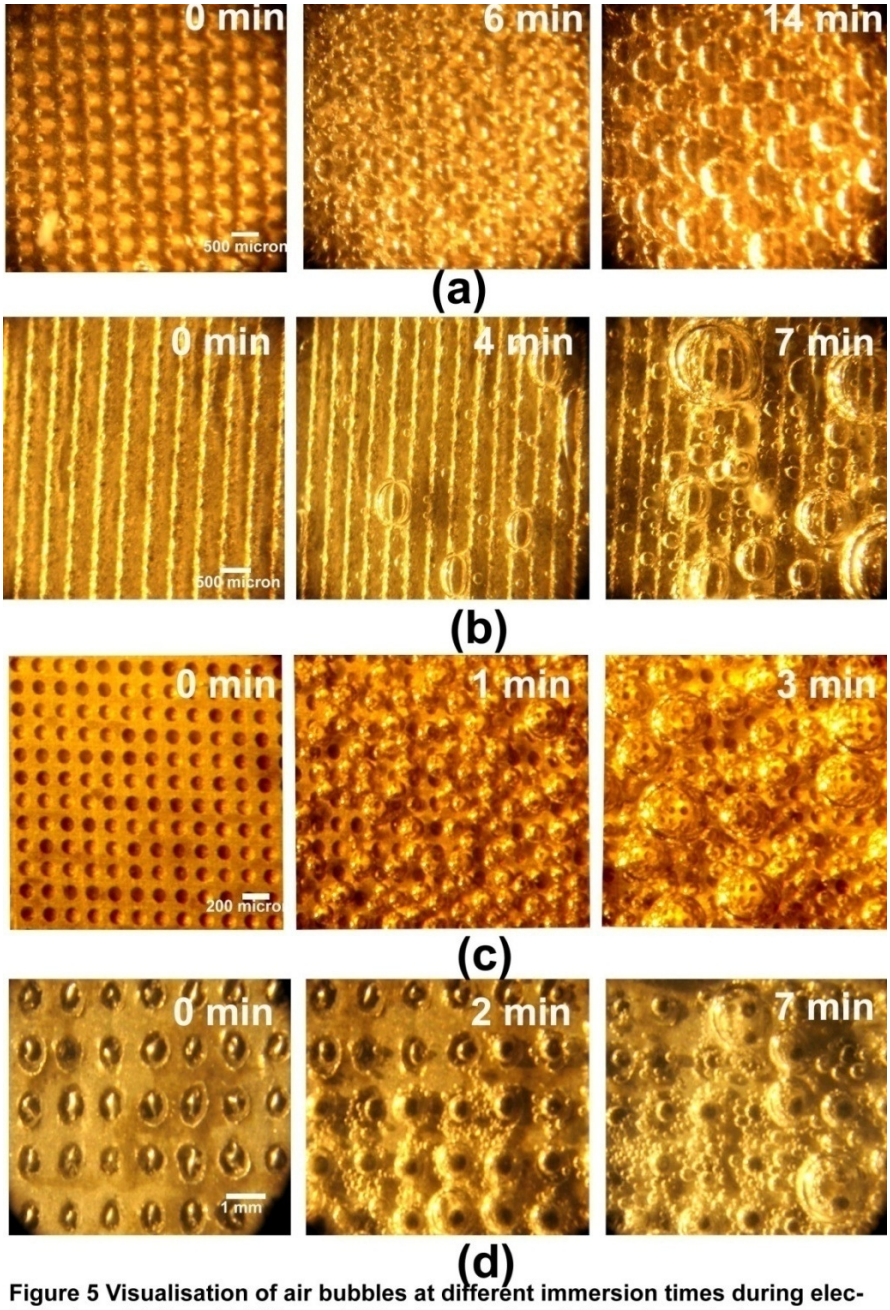

Figure 5 Visualisation of air bubbles at different immersion times during electrolysis : a) Pillars b) Ridges c)100 micron holes d) 500 micron holes

It was seen that the generation of gas bubbles on the surfaces with pillars (Fig 5a) and ridges (Fig 5b) were random in nature. In the surface containing holes (Fig 5c & 5d), small gas bubbles nucleated everywhere on the surface and as they grew they coalesced with each other. These bubbles fed the already trapped larger bubbles in the hole causing them to grow faster. In all the textures, the bubbles departed from the surface upon reaching a critical size with a smaller bubble left behind trapped in the texture. This bubble acted as the nucleus for the next cycle of bubble growth and departure. Thus, the presence of a localized air layer on surface is ensured even when a bubble departs.

4. Conclusions

The air retaining capacities of hydrophobic surfaces with different surface texture has been studied using total internal reflection. The surfaces with holes were most effective in trapping the air under water but the number of air pockets on the surfaces was found to decrease with the immersion time due to diffusion of air into water. Surfaces with larger holes, consequently retaining larger bubbles, were able to retain the Cassie state of wetting the longest. Such surfaces will present a smaller solid fraction to a flow, thereby producing improved drag reductions.

Electrolysis of water can be a viable option for generation of gas to retain the heterogeneous wetting on surfaces for an infinite amount of time provided the surface texture promotes growth of a continuous stable air layer.

References

Bico, J.; Marzolin, C.; Quere, D. *Europhys. Lett.,* **1999**, 47 (2), 220.
Bobji M.S.,;S.V.Kumar; Asthana A; R. N. Govardhan *Langmuir* **2009,** *25(20), 12120*
Callies,. M.; Quere, D. *Soft Matter* **2005**, 1, 55.
Cao, L.; Hu, H.; Gao, D. *Langmuir* **2007,** *23,* 4310.
Cheng, Y-T.; Rodak, D.E. *App. Phys. Lett.***2005**, 86, 144101.
Choi, C.; Westin, K.J.A.; K.S. Breuer, K.S. *Phys. Fluids* **2003,** 15, 2897.
Epstein, P.S.; Plesset, M.S.; *J. Chem. Phys.* **1950**, 18(11), 1505.
Govardhan, R.N.; Srinivas, G.S.; Asthana, A.; Bobji, M.S. Communicated to *Phys. Fluids* **2009.**
Herminghaus, S. *Europhys. Lett.,* **2000**, 52 (2), 165.
Larmour, I.A.; Bell, S.E.J.; Saunders, G.C. *Agnew. Chem. Int. Ed.* **2007**, 46, 1.
Lauga, E.; Stone, H.A.; *J. Fluid Mech.* 2003, **489**, 55.
Lee, C. ; Choi, C. ; Kim, C. *Phys. Rev. Lett.* **2008**, 101, 064501.
Liebermann, L. *J. Applied Phys.* **1957**, 28, 205.
Liu, Y.; Chen, X.; Xin, J. H. *Bioinsp. Biomim.* **2008**, 3, 046007.
Murmur, A. *Langmuir* **2006**, 22, 1400.
Neinhuis, C.; Barthlott, W.; *Annals of Botany* **1997**, 79, 667.
Ou, J.; Perot, B.; Rothstein, J.P. *Phys. Fluids* **2004,** 16, 4635.
Pierre Joseph, Patrick Tabeling . *Physical Review* 2005 E 71, 035303
Sakai, M.; Yanagisawa, T.; Nakajima, A.; Kameshima, Y.; Okada, K. *Langmuir* **2009**, 25,13.
Shibuichi, S.;Onda, T.; Satoh, N.; Tsujii, K. *J. Phys. Chem.* **1996,** *100,* 19512.
Truesdell, R.; Mammoli, A.; Vorobieff, P. ; van Swol, F. ; Brinker, C.J.; *Phys. Rev. Lett.* **2006**, 97, 044504.
Yoshimitsu, Z.; Nakajima, A.; Watanabe, T.; Hashimoto, K. *Langmuir* **2002,** *18,* 5818.
Zhang,J.; Sheng, X.; Jiang, L. *Langmuir* **2009,** *25,* 1371.